Friction

Research Article

Study on the protein adsorption and its properties of self-assembled chitosan coating

Deke Ma[1], Ziyan Zheng[1], Shanhua Qian[1,2,✉], Weiwei Chen[1], Da Bian[1], Zifeng Ni[1]

Cite this article: Ma DK, Zheng ZY, Qian SH, et al. *Friction* 2025, **13**(11): 9441074. https://doi.org/10.26599/FRICT.2025.9441074

ABSTRACT: The protein adsorption properties and biocompatibility of common soft materials often cannot satisfy the functional requirements in the field of cell culture and biological diagnosis. The preparation of a polyelectrolyte coating on the surface of materials is an effective means to solve this problem. Owing to its excellent cell affinity and bioadhesion, chitosan has become an excellent carrier in the biomedical field. Therefore, a polyelectrolyte coating of polydopamine and polyacrylic acid was prepared by polymerization and codeposition under acidic conditions, and the self-assembly of chitosan was carried out on the polyelectrolyte coating to investigate the factors that affect the protein adsorption performance. The study demonstrated that the chitosan coating has outstanding wetting performance, with a 57.54% reduction in the water contact angle after modification. Furthermore, protein adsorption on the original surface was significantly improved. The surface protein adsorption capacity increased with increasing chitosan content, and the maximum adsorption capacity was 4.43 times greater than that of the uncoated sample. Additionally, the chitosan coating had remarkable biocompatibility. The survival rate of mouse osteoblasts cultured on the modified material was 35% greater than that of the original material, and cell proliferation was promoted. The fabrication tactic in this study allows the preparation of chitosan coatings on the polyelectrolyte coating of various material surfaces with controllable surface properties and provides new insights into the preparation tactic of biological coatings for protein adsorption.

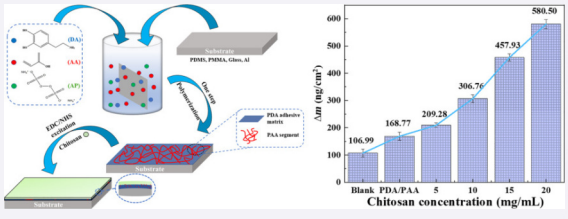

KEYWORDS: chitosan; protein adsorption; biocompatibility; polymerization and codeposition tactics

1 Introduction

In the field of medical inspection, interactions between instrument surfaces and proteins are very important [1–3]. In the medical fields of biomolecule separation, biodetection, and carrier materials require excellent biocompatibility and protein adsorption capabilities without destroying the natural conformation and biological functions of adsorbed proteins [4–6].

The surface of the polyelectrolyte coating reduces the conformational stability of the adsorbed protein, which attracts biomolecules such as proteins with opposite charges, meeting the needs of biomedical materials [7–9]. Polyelectrolytes are polymers with repeating units containing electrolyte groups, and their application and development in sensor devices, supercapacitors, new batteries, actuators, catalysis, and other fields are evident [10–12]. Chitosan is a positively charged natural polyelectrolyte. Its primary amine group is very active and can provide reaction sites for various reactions [13]. Moreover, owing to its advantages of good bioadhesion, natural renewability, and low cost, chitosan can be widely used in the field of biomedicine [14, 15].

The simplest method to prepare a chitosan coating on a substrate is physical adsorption, such as impregnation or spin coating. However, these methods lack stability and cohesiveness [16]. Compared with physical adsorption methods, covalent adsorption can yield tenfold stronger adhesion [17]. Dopamine (DA) has garnered significant attention because of its ability to adhere to various materials and mild reaction conditions [18]. It can be characterized by excellent adhesion, biocompatibility, and chemical activity, and can be deposited on any surface [19–21]. Furthermore, catechol and its derivatives in DA can be grafted onto chitosan, making it a common choice to enhance the adhesion properties [16]. However, for most chitosan and its derivative coatings prepared from dopamine, the arm connection of hydrocaffeic acid was first obtained. The amino group of chitosan can then be coupled by activating the carboxyl group to achieve covalent adsorption [22, 23].

Alternatively, coating substrates with chitosan after plasma treatment with gases such as acrylic acid (AA) eliminates the need to connect the arm, but the substrate needs special pretreatment, and the corresponding cost is high [24]. Typically, the fabrication method for creating polymer coatings on material surfaces has the following characteristics under mild reaction conditions:

[1] School of Mechanical Engineering, Jiangnan University, Wuxi 214122, China. [2] Jiangsu Key Laboratory of Advanced Food Manufacturing Equipment and Technology, Jiangnan University, Wuxi 214122, China.

✉ Corresponding author. E-mail: qiansh@jiangnan.edu.cn

Received: August 28, 2024; Revised: December 20, 2024; Accepted: February 1, 2025

biocompatibility, simple processing, strong adhesion, and substrate independence [25]. Self-assembly technology is a common and simple coating technique that is based mainly on the interaction between different coatings to construct new composite coatings [26, 27]. The coating prepared via the self-assembly technique is expected to be suitable for the special process of polyelectrolyte coating.

In our previous work, the polymerization codeposition tactic under acidic surroundings was discussed, and polydopamine (PDA) composite coatings were prepared on the surface of four materials [28], which also provided new insights into the preparation of chitosan coatings. To design the ideal process of self-assembled chitosan coating with a PDA composite coating as the intermediate layer, this study was carried out. The PDA/polyacrylic acid (PAA) coating was used as the intermediate layer to self-assemble the chitosan coating; the factors influencing the surface properties, such as the protein adsorption of the chitosan coating, were determined, and the biocompatibility of the coating was also evaluated. This study can serve as a novel reference for the development of medical protein detection devices.

2 Experimental

2.1 Experimental materials

Dopamine hydrochloride (98%), 1-ethyl-(3-dimethylamino-propyl) carbodiimide hydrochloride (EDC, 98.5%), chitosan ($(C_6H_{11}NO_4)_n$, degree of deacetylation 95%), and ammonium persulfate ($(NH_4)_2S_2O_8$, 99%) were obtained from Macklin Biochemical Technology Co. Acetic acid (CH_3COOH), acrylic acid (AA, 99%) and N-hydroxysuccinimide (NHS, 97%) were obtained from Sinopharm Chemical Reagent Co.

Since protein is a relatively viscous molecule, other components in the protein solution nonspecifically bind to the matrix during the detection process, which greatly interferes with the tests. Bovine serum albumin (BSA) can prevent nonspecific binding of impurities to the substrate and improve the reliability of the results. Therefore, BSA solutions were used to characterize the protein absorption of the coating and were obtained from Sangon Bioengineering Co. Mouse osteoblasts (MC3T3-E1), α-MEM medium, and Cell Counting Kit-8 (CCK-8 reagent) were purchased from Beyotime Biotechnology Co. Sodium hydroxide (NaOH, 97%) was also purchased from Sinopharm Chemical Reagent Co. 0.01 M phosphate-buffered saline (PBS) and 0.03 M 4-morpholineethanesulfonic acid (MES) were used as buffer solutions.

Polydimethylsiloxane (PDMS) has excellent physiological inertia and does not significantly cause adverse reactions in human tissues; thus, it has been widely used in various medical devices that directly contact the human body. Therefore, PDMS (Sylgard 184, Dow Corning) was selected as the substrate and was prepared with a 10:1 mass ratio of the base component to the curing agent [6]. Other substrates (QCM chips, glass slides, aluminum sheets, and polymethyl methacrylate (PMMA)) were all commercially available products. The test water used was deionized water.

2.2 Preparation of the chitosan coating

First, DA and AA were separately added to deionized water, after which the pH of the mixed solution was adjusted to 5.5. After thorough mixing, the ammonium persulfate solution was added gradually. The mixed solution was heated in a water bath (45 °C) for approximately 12 h. After washing and drying, the PDA/PAA coating was obtained. Then, chitosan was dissolved in 2% acetic acid solution, and the pH of the solution was adjusted to 4.5 [29].

EDC is a common activator of the carboxyl group. The coating was soaked in EDC solution to activate the carboxyl groups on the surface and improve the surface activity of the coating. However, the activated products were prone to hydrolysis, and NHS was generally used to further react to form stable esters. Therefore, EDC/NHS was selected as the pretreatment solution. After complete dissolution, the substrate coated with PDA/PAA was soaked in EDC/NHS solution for 1 h at low temperature and then immersed in the chitosan solution for approximately 3 h.

The substrate was subsequently thoroughly washed with deionized water, and the work was carried out after drying. The preparation process is shown in Fig. 1. The concentrations of DA and AA were maintained at 2 and 4 mg/mL, respectively. The

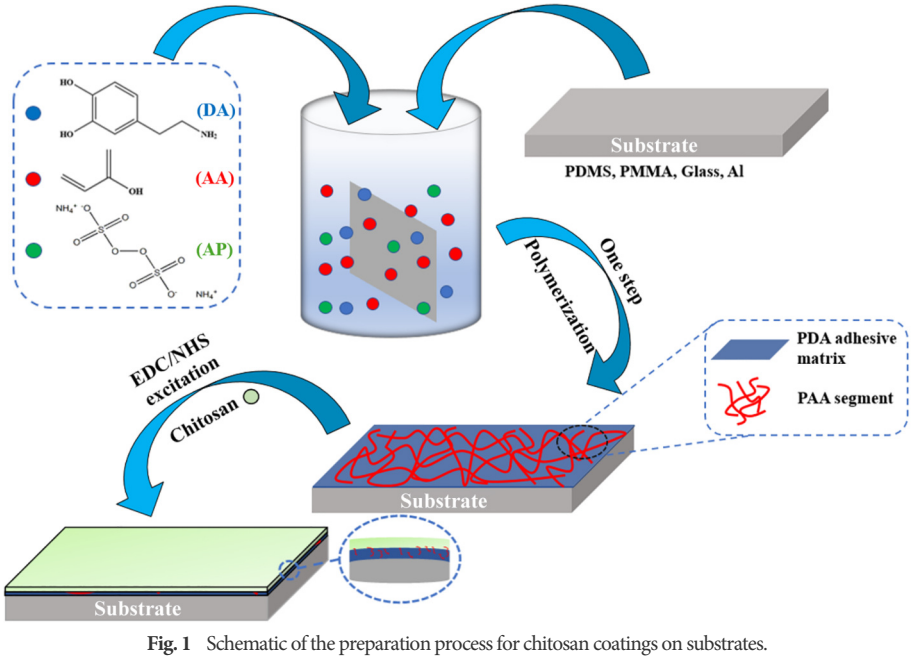

Fig. 1 Schematic of the preparation process for chitosan coatings on substrates.

chitosan concentration was selected at four concentrations of 5, 10, 15, and 20 mg/mL.

2.3 Characterization of surface properties

The functional groups on the surface of the PDMS were analyzed via a Fourier transform infrared (FTIR) spectrometer (Nicolet iS10, Thermo Fisher Scientific, USA). The morphology of the elements on the PDMS surface was characterized via an energy-dispersive X-ray spectrometer (EDS; Zeiss Sigma HD, Carl Zeiss, Germany) and a scanning electron microscope (SEM; Zeiss Gemini Sigma 300 VP, Carl Zeiss, Germany).

The coating roughness and thickness were characterized via a white light interferometer (MFP-D, RTEC, USA). Notably, the coating thickness was the critical point between the coating and the substrate according to the MFP-D and was obtained via the data processing method. In addition, the surface wettability of the coatings was characterized via a contact angle measurement instrument (Powereach, China). During the whole experiment, the volume of all the droplets was 2 μL.

The protein adsorption performance of the coatings was analyzed via a dissipative quartz crystal microbalance (QCM-D; Q-Sense Analyzer, Biolin Scientific, Sweden) at 25 °C to characterize the dynamic frequency of the coated QCM chip. Since protein is a relatively viscous molecule, other components in the protein solution nonspecifically bind to the matrix during the detection process, which greatly interferes with the tests. The BSA can prevent nonspecific binding of impurities to the substrate and improve the reliability of the results [30]. Therefore, BSA solutions were used to characterize the protein absorption of the coating, and were obtained from Sangon Bioengineering Co. PBS solution was introduced into the instrument for calibration. After stabilization, the solution containing 1 mg/mL BSA was injected for 1 h. After adsorption was complete, the unbound protein was removed in PBS, and the mixture was incubated for 20 min. In this study, according to the Sauerbrey equation [31], the gain/loss mass of the surface was computed by means of the relationship between the frequency and time of the fifth overtone generation:

$$\Delta m = -\frac{C\Delta f}{n} \tag{1}$$

where Δm is the absorbed protein mass; C is the mass sensitivity constant (17.7 ng/(cm^2·Hz)); Δf is the frequency difference; n is the overtone number.

2.4 Evaluation of the biocompatibility

The biocompatibility of the prepared coatings was estimated via the MC3T3-E1 cell activity method. The medium was used as the extraction medium, and the medium was soaked in a constant-temperature oscillator at 37 °C for 72 h. The extraction ratio was 1 mL/cm^2. Each well was inoculated into a sterile 96-well plate at a density of 5×10^3 cells. After the cells were completely adherent, the original culture medium was removed, and 100 μL of extraction solution containing different samples was added to each well. The cells cultured without the sample extract were set as the control group, and the cells without cells were set as the blank group. The 96-well plates containing the added sample extraction solution were placed in the incubator for 24, 48, or 72 h. Afterward, the culture medium inside the wells was removed, and 100 μL of 10% CCK-8 reagent was added to each well and incubated at 37 °C for 1 h.

The absorbance of each well at a wavelength of 450 nm was measured via a microplate reader (Spectra MAX, Molecular Devices, USA), and the cell survival rate of each test group was calculated using Eq. (2):

$$\text{Cell viability} = \frac{A_e - A_b}{A_p - A_b} \times 100\% \tag{2}$$

where A_e is the absorbance reading of the wells in the testing group; A_p is the absorbance reading of the wells in the control group; A_b is the absorbance reading of the wells in the blank group (background absorbance of the plate). To analyze the differences in cell activity on different surfaces more clearly and intuitively, the cytoskeleton and nucleus were stained, and cell adhesion was observed via a laser confocal microscope (LSM880, Carl Zeiss, USA) after the surfaces of different extracts were amplified 40 times.

3 Results and discussion

3.1 Composition of the coating surface

Figure 2 shows the infrared spectra of the PDMS, PDA/PAA, and chitosan coatings. The main chain from the PDMS is composed of silicon and oxygen atoms connected by silicon–oxygen bonds, and the side chain consists of methyl groups [28]. The peaks at 2,962, 1,260, and 795 cm^{-1} are attributed to Si–CH_3 asymmetric stretching vibration absorption, Si–CH_3 twisting deformation vibration absorption, and Si–CH_3 stretching vibration absorption, respectively. The peaks at 1,074 and 1,019 cm^{-1} are both attributed to the asymmetric stretching of Si–O–Si [32, 33]. The stretching vibration absorption peaks of –NH_2 and –OH appeared at 3,380

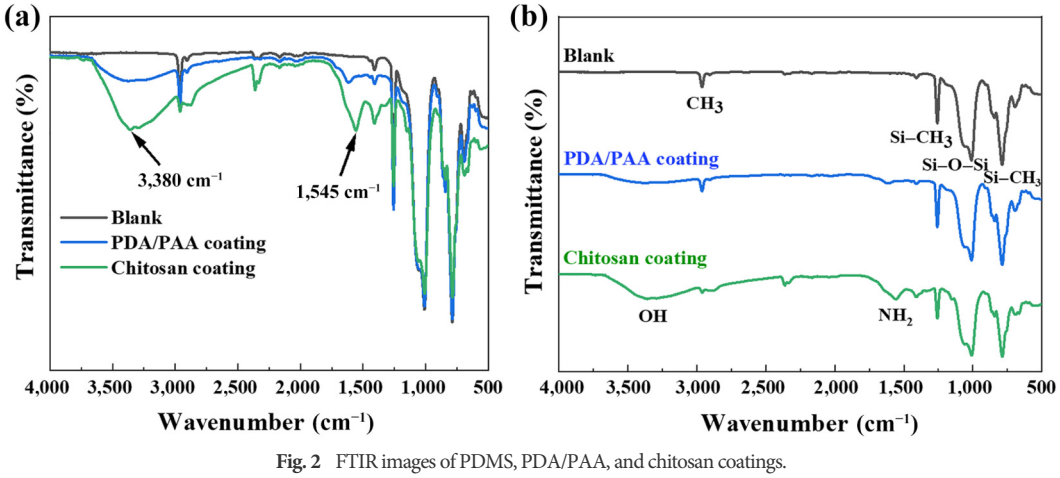

Fig. 2 FTIR images of PDMS, PDA/PAA, and chitosan coatings.

and 1,545 cm^{-1} on the surface of the PDMS after DA/AA polymerization deposition [34]. The absorption peaks of $-NH_2$ and –OH are more significant after the self-assembly of chitosan from the PDA/PAA coating surface, which is consistent with the reported spectral peaks of chitosan [35].

To determine the composition of the prepared surfaces further, EDS elemental analysis was carried out. As listed in Table 1, the nitrogen (N) content on the PDMS surface is positively correlated with the chitosan concentration, reaching a maximum value of 3.61% at a chitosan concentration of 20 mg/mL. Moreover, the silicon (Si) content decreased with increasing chitosan concentration, with the lowest Si content of 20.62% observed at the highest chitosan concentration. This trend is due to the increased covalent adsorption of chitosan on the PDA/PAA coating surface with increasing chitosan concentrations. This led to an increasing N content and a decreasing Si content on the PDMS surface. Through FTIR and EDS analyses, it was proven that the chitosan coating was superiorly prepared on the PDMS surface.

3.2 Surface morphology of the coatings

Figure 3 shows the surface morphology before and after coating at 2,000× magnification. Compared with those on the untreated PDMS surface (Fig. 3(a)), the numerous small particles on the PDMS coating surface (Fig. 3(b)) are due primarily to the decrease in the adhesion of aggregates with the addition of AA. The DA/AA was polymerized by the AP and deposited into relatively large particles, and it could bond to the PDMS surface with enough DA adhesion sites [26]. As shown in Figs. 3(e) and 3(f), with increasing chitosan concentration, larger particles appeared on the surface of the PDMS, making it much rougher. To validate the trends of surface roughness (Ra) and thickness of the chitosan coatings with increasing concentration, characterization is needed.

Figure 4 shows the surface elemental content and distribution after self-assembly at a chitosan concentration of 20 mg/mL. The distribution diagram shows that the surface of the chitosan coating was mainly composed of four elements, C, N, O, and Si, and the distribution of component elements on the surface was homogeneous.

As shown in Fig. 5(a), the untreated PDMS surface has the smallest Ra of 14.28 nm, which increases to 31.56 nm because of the PDA/PAA coating. The surface roughness of the PDMS increased after DA/AA polymerization. When chitosan was polymerized on the surface through the PDA/PAA intermediate layer, the small PDA/PAA particles were covered by chitosan at low concentrations, which reduced the surface roughness of the composite coating. The surface roughness of the composite coating increased with increasing chitosan concentration. As the concentration of chitosan increased, it first decreased but then increased. At a chitosan concentration of 20 mg/mL, the Ra reached a maximum of 71.97 nm, which was 4.04 times greater than that of the untreated PDMS surface. This trend almost aligns with the observed surface morphology in the SEM images.

Figure 5(b) shows the variation in coating thickness with different chitosan contents. The thickness of the coating was positively correlated with the chitosan concentration, reaching 149.65 nm at a chitosan concentration of 20 mg/mL, representing an increase of 75.79% compared with the thickness of the PDA/PAA coating. These results further confirm the positive correlation between the amount of chitosan self-assembled on the

Table 1 Elemental content of PDMS surface after coating with different chitosan concentrations (Unit: wt%)

Chitosan concentration	C	N	O	Si
PDMS	27.21	0	33.13	39.66
PDA/PAA coating	32.94	1.00	32.28	33.78
5 mg/mL	37.93	1.16	28.26	32.65
10 mg/mL	36.24	1.37	30.4	31.99
15 mg/mL	41.16	2.06	27.08	29.7
20 mg/mL	45.28	3.61	30.49	20.62

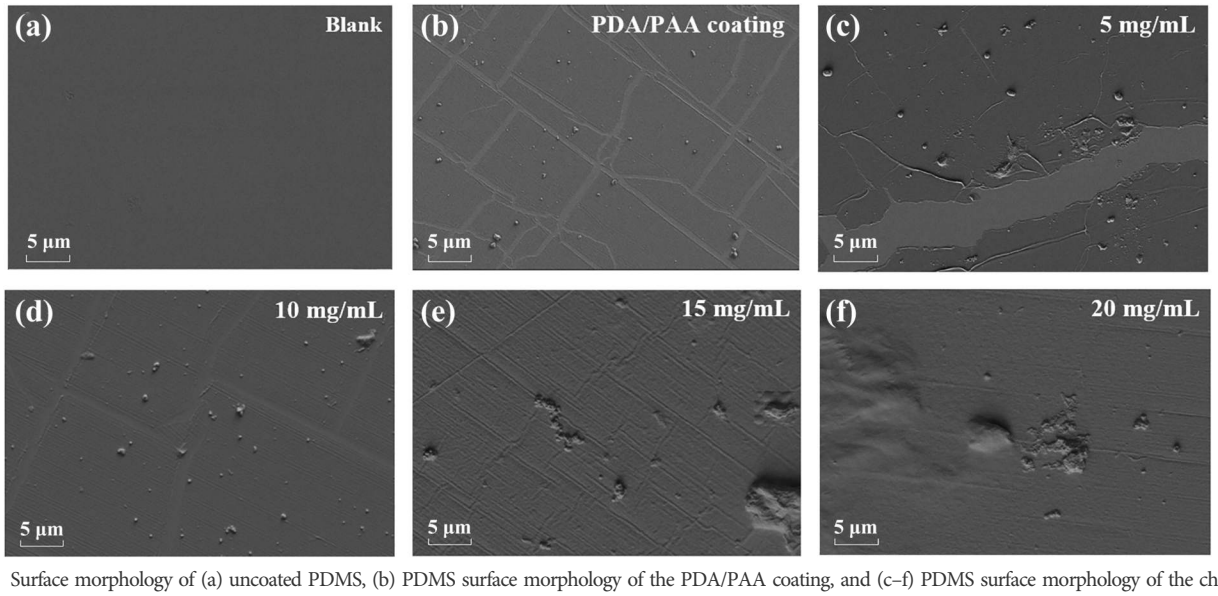

Fig. 3 Surface morphology of (a) uncoated PDMS, (b) PDMS surface morphology of the PDA/PAA coating, and (c–f) PDMS surface morphology of the chitosan coating at different concentrations.

PDA/PAA coating and the chitosan concentration, which is consistent with previous results. The thickness of the self-assembled chitosan coating was regulated by controlling the concentration of the chitosan solution to meet the requirements of different applications.

3.3 Wettability of the coating

Excellent wettability is essential to prevent adverse effects such as conformational changes in proteins adsorbed on the surface. Investigating surface wettability is highly important for biomedical materials in the field of protein adsorption. As shown in Fig. 6(a), the uncoated PDMS had a water contact angle (WCA) of 117.09°, and its surface was hydrophobic, which significantly decreased after the preparation of the DA/PAA coating. However, as the chitosan concentration increased, the WCA of the coating surface initially increased but then decreased. This may be due to the possibility that the wettability of the chitosan coating is weaker than that of the PDA/PAA coating. At a chitosan concentration of 20 mg/mL, the surface WCA was 57.54% lower than that of the untreated surface. This is mainly because the chitosan coating includes many hydrophilic groups with strong hygroscopicity, which can bind many water molecules and enhance wettability

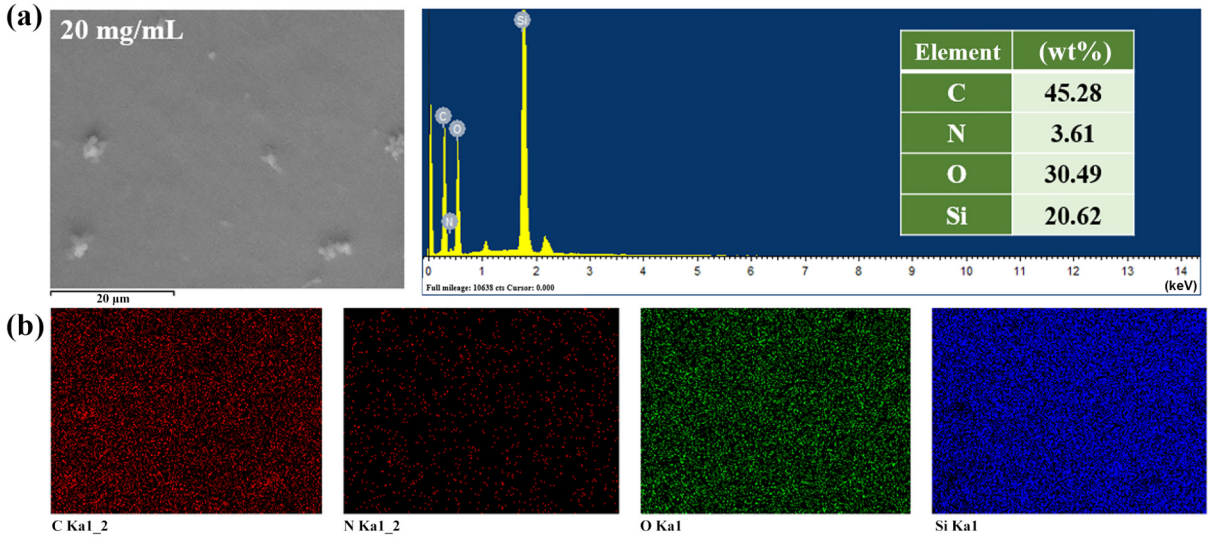

Fig. 4 (a) Surface elemental content and (b) distribution map after self-assembly at a chitosan concentration of 20 mg/mL.

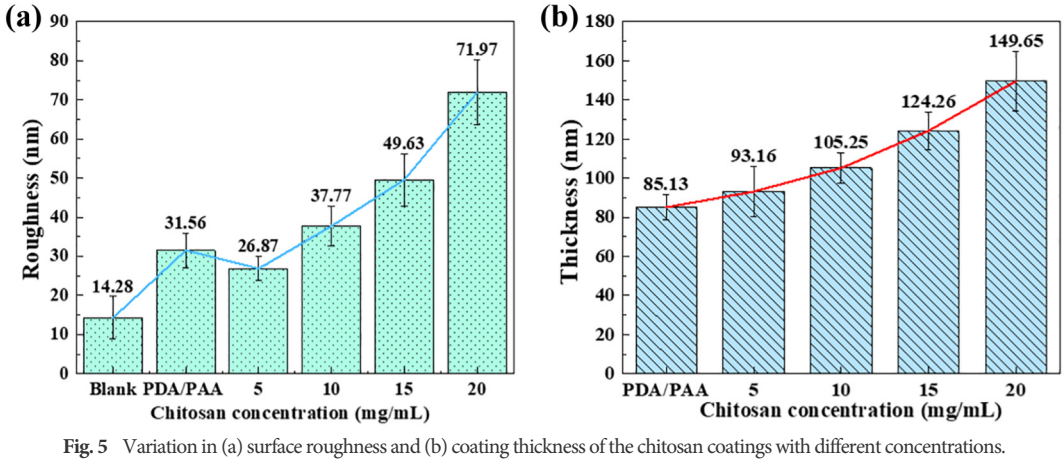

Fig. 5 Variation in (a) surface roughness and (b) coating thickness of the chitosan coatings with different concentrations.

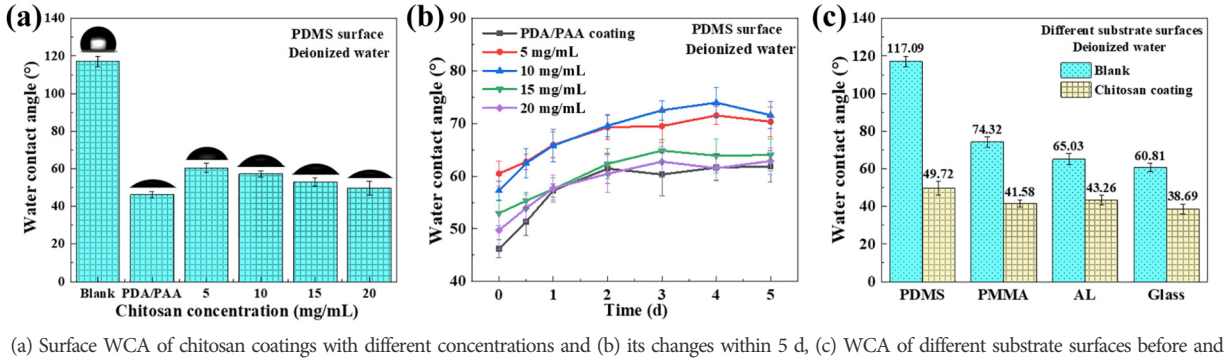

Fig. 6 (a) Surface WCA of chitosan coatings with different concentrations and (b) its changes within 5 d, (c) WCA of different substrate surfaces before and after chitosan coating.

[36]. Moreover, based on the Wenzel model [37], surface roughness affects surface wettability to some extent:

$$\cos\theta = R_f \cos\theta_0 \quad (3)$$

where θ is the WCA on the actual surface; R_f is the special factor proportional to the roughness; θ_0 is the WCA on the initial surface. When θ_0 decreases below 90°, as the surface roughness increases, the surface wettability also increases [38]. Therefore, when increasing the chitosan content results in increasing surface roughness, the WCA decreases gradually.

Figure 6(b) illustrates the variation trend of the WCA over time for the coatings. Both the PDA/PAA and chitosan coatings showed a consistent trend in which the WCA slowly increased within 2 days and then stabilized. This is probably because the hydrophobic functional groups in the coating tend to move closer to the surface to reduce the surface energy [39].

The results indicated that the chitosan coating maintained favorable wettability even after these coatings were bare for 5 days under air. Furthermore, the chitosan coating preparation strategy in this study is independent of the substrate. Furthermore, the chitosan coating preparation strategy in this study can be applied to a wide range of substrates.

Figure 6(c) shows the WCA before and after coating on PDMS, PMMA, aluminum, and glass. The results demonstrated that the chitosan coating effectively covered the surfaces of all four substrates and that their wettability properties were significantly enhanced.

3.4 Coating properties related to protein adsorption

Figure 7 shows that protein adsorption on the QCM chip increased after PDA/PAA deposition. With increasing chitosan concentration, the protein adsorption capacity tends to increase. With a chitosan content of 20 mg/mL, the protein adsorption capacity of the coating was 580.50 ng/cm^2, which was 4.43 times greater than that of the initial chip surface. This suggests that one of the kernel factors affecting protein adsorption on the surface is electrostatic interactions [3]. BSA has an isoelectric point of approximately 4.8 and has a negative charge under weakly acidic conditions (pH = 6) [40]. On the other hand, chitosan is a naturally occurring electrolyte with a positive charge [13]. It can adsorb a large amount of BSA through electrostatic interactions. The amount of chitosan adsorbed on the PDA/PAA coating was positively related to the chitosan content, the positive charge on the coating surface also increased, and the electrostatic interaction ability increased, thereby increasing protein adsorption. In addition, previous studies have shown a close relationship between protein adsorption and surface roughness. Surfaces with greater surface roughness have greater protein adsorption capacity [41, 42]. An increase in the amount of chitosan and surface roughness on the material surface can increase the ability of the material surface to adsorb protein, which can meet the requirements of the carrier surface for protein adsorption. The main factors influencing protein physical adsorption are hydrophobic and electrostatic forces. In addition, when the surface of a material is modified mainly by acids, the hydrophobic forces have less influence than the electrostatic forces. The presence of acid groups can increase surface hydrophilicity and reduce surface hydrophobicity, thus reducing the influence of hydrophobic forces on protein adsorption.

3.5 Water stability performance of the coating

Figure 8 shows the variation in the WCA and thickness of the chitosan coatings after they were immersed in water for 72 h. After the immersion, the WCA of the coating tends to be stable, and the maximum change value is less than 5°, and there is no significant increase. Even after 5 days of immersion, the WCA remained significantly lower than that of the original surface. The change in thickness of the chitosan coating after immersion for 72 h was less than 10 nm, and the change in thickness was far less than the initial thickness. These results indicate that the original wettability and thickness of the chitosan coating can be maintained after immersion for 72 h and that the coating can self-assemble on the PDA/PAA surface firmly and stably. Even after they were immersed, they still exhibited excellent surface

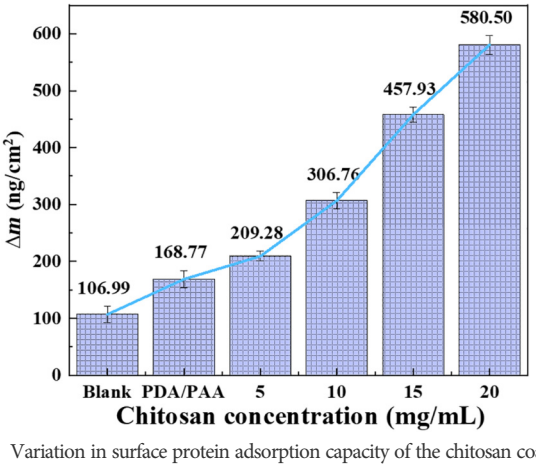

Fig. 7 Variation in surface protein adsorption capacity of the chitosan coatings with increasing chitosan concentration.

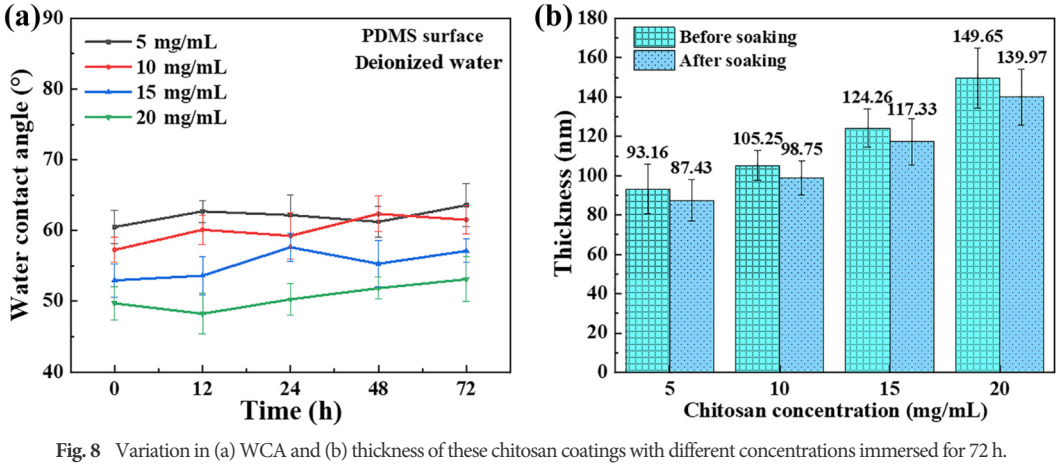

Fig. 8 Variation in (a) WCA and (b) thickness of these chitosan coatings with different concentrations immersed for 72 h.

performance, demonstrating the excellent water stability of chitosan. This suggests that it can be used for surface modification in material applications in aqueous environments [43].

3.6 Biocompatibility of the coatings

Figure 9 shows the viability of MC3T3-E1 cells cultured with the PDMS extract before and after coating for 72 h. The viability of MC3T3-E1 cells was negatively correlated with the culture time of the PDMS extract. When they were cultured for 72 h, the cell viability decreased to 67%, which was significantly lower than that of the control group (100%). These findings indicate that PDMS has a certain degree of toxicity and that the toxic substances extracted by immersion greatly affect the normal activity of cells. Nevertheless, the viability of MC3T3-E1 cells was positively correlated with the culture time of the PDMS extract after chitosan coating. When the mixture was cultured for 24 h, the cell viability was 96%, which was much greater than the 86% viability of the PDMS extract. The chitosan coating exhibited excellent biocompatibility and considerably inhibited the release of toxic substances from the PDMS. When they were cultured for 72 h, the cell viability increased to 102%, which was even greater than the 100% of the control group. These findings suggest that the chitosan coating not only has excellent biocompatibility but also promotes cell proliferation.

Chitosan can promote cell proliferation, mainly because of its special characteristics. The macromolecular structure of chitosan includes many amino and hydroxyl groups. These functional groups interact with the molecules on the cell surface to provide suitable growth surroundings for the cells, thus promoting cell adhesion and proliferation to a certain extent [44]. Figure 10 shows the degree of cell adhesion on the surfaces of the normal culture medium, PDMS extract, and chitosan coating extract after cultivation for 72 h. The number of adhered cells on the chitosan surface extracted after cultivation for 72 h was significantly greater than that on the extracted PDMS surface and even greater than the number of adhered cells under normal culture conditions, which further confirmed the excellent biocompatibility of the chitosan coating.

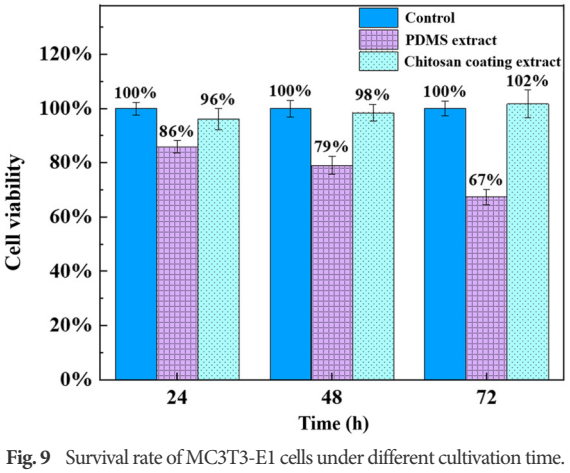

Fig. 9 Survival rate of MC3T3-E1 cells under different cultivation time.

3.7 Discussion

The coatings were prepared on different substrates, and their properties were investigated. It was found that the chitosan coatings could be adsorbed on the surface of various materials. The possible reasons are as follows.

As a natural high-molecular-weight polysaccharide, chitosan has many biological properties and good biocompatibility. The self-assembly of chitosan involves various factors (such as the degree of cationic nature of the material, pH, etc.). Under acidic conditions, the amino groups of chitosan are protonated, resulting in an increasing degree of cationicity, which promotes their interaction with negatively charged surfaces [45]. In acidic aqueous solutions, the cationic and hydrophilic nature of chitosan makes it simple to interact with negatively charged surfaces. The PDA/PAA layer has a large amount of negative charge due to carboxylate ions. Therefore, a stable chitosan coating could be formed on the PDA/PAA surface through electrostatic interactions.

The amino groups in chitosan can spontaneously undergo chemical cross-linking reactions with the quinone groups of PDA through Schiff base and Michael addition reactions [46, 47] (Fig. 11(a)). The carboxylic acid groups from the PAA chains in the interlayer can be activated by EDC/NHS [48, 49] to generate NHS esters, which react readily with the amino groups in chitosan (Fig. 11(b)). This allowed the chitosan to be firmly self-assembled on the material surface by covalent adsorption. In this work, a PDA/PAA interlayer was prepared by polymerization and codeposition tactics in acidic conditions. PDA has abundant catechol functional groups and amino groups and is firmly codeposited on various substrates in a covalent and noncovalent manner with PAA [18]. This approach enables the preparation of chitosan coatings on various material surfaces using a PDA/PAA layer as an interlayer and provides new insights into the preparation strategy for chitosan coatings.

4 Conclusions

(1) Under weakly acidic conditions, we prepared a polydopamine (PDA)/polyacrylic acid (PAA) interlayer, and the ideal surface

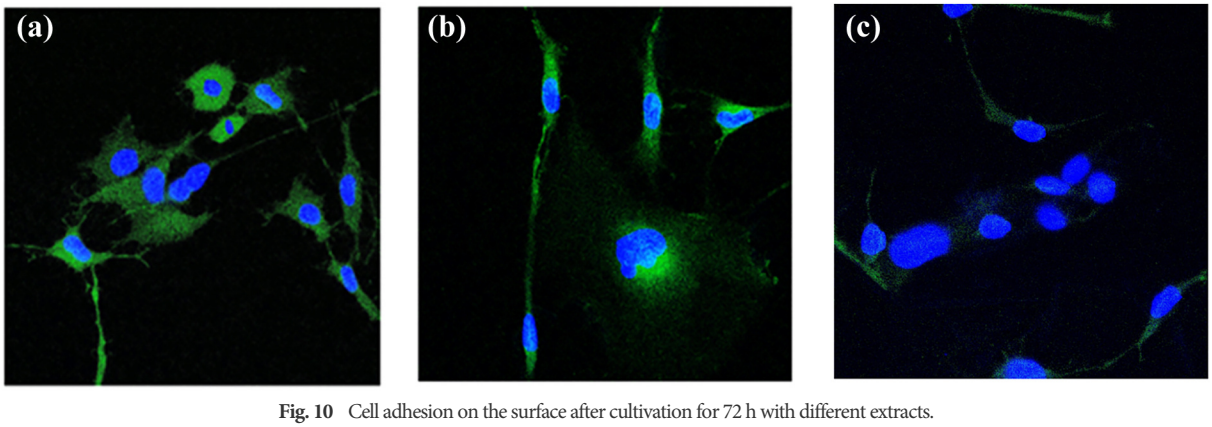

Fig. 10 Cell adhesion on the surface after cultivation for 72 h with different extracts.

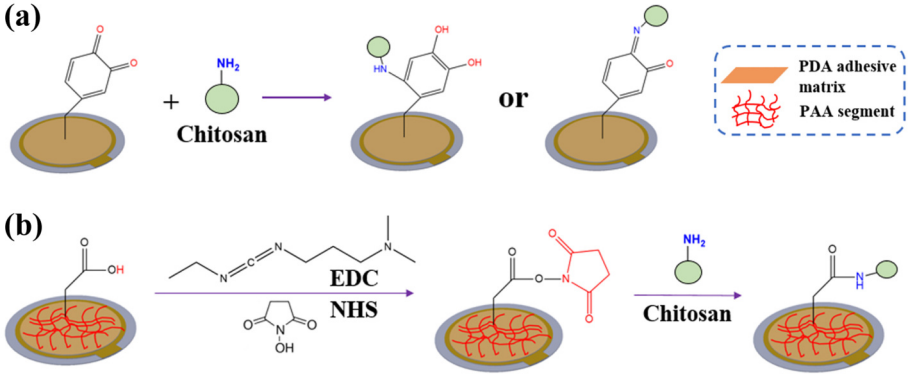

Fig. 11 Schematic diagram of (a) PDA covalent chitosan and (b) PAA covalent chitosan.

used for protein adsorption was prepared via self-assembly of chitosan. The process was substrate independent and suitable for large-scale preparation and application.

(2) Chitosan coatings significantly reduced the water contact angle (WCA) of the substrate surface and had excellent protein adsorption properties. The protein adsorption from this chitosan layer was 580.50 ng/cm^2, which was 4.43 times greater than that of the uncoated sample.

(3) Compared with the original surface, the chitosan coating had excellent biocompatibility and strong water stability, and the survival rate of mouse osteoblasts cultured on the modified surface increased by 35%, which promoted cell proliferation. The coating can be expected to be applied in the medical detection field.

Acknowledgements

The authors acknowledge financial projects from the National Natural Science Foundation of China (No. 52375184) and Jiangsu Key Laboratory of Advanced Food Manufacturing Equipment and Technology (Jiangnan University) (No. FMZ202204).

Declaration of competing interest

The authors have no competing interests to declare that are relevant to the content of this article. The author Shanhua Qian is the Youth Editorial Board Member of this journal.

References

[1] Totani M, Liu L, Matsuno H, Tanaka K. Design of a star-like hyperbranched polymer having hydrophilic arms for anti-biofouling coating. *J Mater Chem B* **7**(7): 1045–1049 (2019)

[2] Wei Q, Becherer T, Angioletti-Uberti S, Dzubiella J, Wischke C, Neffe A T, Lendlein A, Ballauff M, Haag R. Protein interactions with polymer coatings and biomaterials. *Angew Chem Int Ed* **53**(31): 8004–8031 (2014)

[3] Becker A L, Henzler K, Welsch N, Ballauff M, Borisov O. Proteins and polyelectrolytes: A charged relationship. *Curr Opin Colloid In* **17**(2): 90–96 (2012)

[4] Nagase K, Kobayashi J, Kikuchi A, Akiyama Y, Kanazawa H, Okano T. Thermoresponsive anionic copolymer brushes containing strong acid moieties for effective separation of basic biomolecules and proteins. *Biomacromolecules* **15**(10): 3846–3858 (2014)

[5] Li L, Smitthipong W, Zeng H B. Mussel-inspired hydrogels for biomedical and environmental applications. *Polym Chem* **6**(3): 353–358 (2015)

[6] Chen W W, Xu B, Tang Q C, Qian S H, Bian D, Li H. Preparation and properties of PDMS surface coating for ultra-low friction characteristics. *Langmuir* **39**(41): 14605–14615 (2023)

[7] Rabe M, Verdes D, Seeger S. Understanding protein adsorption phenomena at solid surfaces. *Adv Colloid Interface Sci* **162**(1–2): 87–106 (2011)

[8] Welsch N, Lu Y, Dzubiella J, Ballauff M. Adsorption of proteins to functional polymeric nanoparticles. *Polymer* **54**(12): 2835–2849 (2013)

[9] Ye G, Lee J, Perreault F, Elimelech M. Controlled architecture of dual-functional block copolymer brushes on thin-film composite membranes for integrated "defending" and "attacking" strategies against biofouling. *ACS Appl Mater Inter* **7**(41): 23069–23079 (2015)

[10] McShane M J. Enzyme immobilization in polyelectrolyte microcapsules. In: *Enzyme Stabilization and Immobilization*. Minteer S, Ed. Totowa (USA): Humana Press, 2011: 147–154

[11] You J, Park T, Kim J, Heo J S, Kim H S, Kim H O, Kim E. Highly fluorescent conjugated polyelectrolyte for protein sensing and cell-compatible chemosensing applications. *ACS Appl Mater Inter* **6**(5): 3305–3311 (2014)

[12] Han L B, Yan B, Zhang L, Wu M, Wang J Y, Huang J, Deng Y H, Zeng H B. Tuning protein adsorption on charged polyelectrolyte brushes *via* salinity adjustment. *Colloid Surface A* **539**: 37–45 (2018)

[13] Hu L M, Sun Y, Wu Y. Advances in chitosan-based drug delivery vehicles. *Nanoscale* **5**(8): 3103 (2013)

[14] Wang H X, Qian J, Ding F Y. Recent advances in engineered chitosan-based nanogels for biomedical applications. *J Mater Chem B* **5**(34): 6986–7007 (2017)

[15] Zhang Y D, Li L, Yu C H, Hei T T. Chitosan-coated polystyrene microplate for covalent immobilization of enzyme. *Anal Bioanal Chem* **401**(7): 2311–2317 (2011)

[16] Campelo C S, Chevallier P, Loy C, Vieira R S, Mantovani D. Development, validation, and performance of chitosan-based coatings using catechol coupling. *Macromol Biosci* **20**(1): 1900253 (2020)

[17] Martin H J, Schulz K H, Bumgardner J D, Schneider J A. Enhanced bonding of chitosan to implant quality titanium via four treatment combinations. *Thin Solid Films* **516**(18): 6277–6286 (2008)

[18] Lee H, Dellatore S M, Miller W M, Messersmith P B. Mussel-inspired surface chemistry for multifunctional coatings. *Science* **318**(5849): 426–430 (2007)

[19] Zhu L P, Jiang J H, Zhu B K, Xu Y Y. Immobilization of bovine serum albumin onto porous polyethylene membranes using strongly attached polydopamine as a spacer. *Colloid Surface B* **86**(1): 111–118 (2011)

[20] Liu R R, Chen Q, Cao M Y, Lin J Y, Lin F, Ye W Y, Luis P, Van der Bruggen B, Zhao S F. Robust bio-inspired superhydrophilic and underwater superoleophobic membranes for simultaneously fast water and oil recovery. *J Membr Sci* **623**: 119041 (2021)

[21] Saiz-Poseu D J, Mancebo-Aracil D J, Nador D F, Busqué D F, Ruiz-Molina D D. The chemistry behind catechol-based adhesion. *Angew Chem Int Ed* **58**(3): 696–714 (2019)

[22] Kim K, Shin M, Koh M Y, Ryu J H, Lee M S, Hong S, Lee H. TAPE: A medical adhesive inspired by a ubiquitous compound in plants. *Adv Funct Mater* **25**(16): 2402–2410 (2015)

[23] Ghadban A, Ahmed A S, Ping Y, Ramos R, Arfin N, Cantaert B, Ramanujan R V, Miserez A. Bioinspired pH and magnetic responsive catechol-functionalized chitosan hydrogels with tunable elastic properties. *Chem Commun* **52**(4): 697–700 (2016)
[24] Ferreira A M, Carmagnola I, Chiono V, Gentile P, Fracchia L, Ceresa C, Georgiev G, Ciardelli G. Surface modification of poly (dimethylsiloxane) by two-step plasma treatment for further grafting with chitosan–Rose Bengal photosensitizer. *Surf Coat Tech* **223**: 92–97 (2013)
[25] Wei Q B, Liu X Q, Yue Q Y, Ma S H, Zhou F. Mussel-inspired one-step fabrication of ultralow-friction coatings on diverse biomaterial surfaces. *Langmuir* **35**(24): 8068–8075 (2019)
[26] Fan Q Q, Ma J Z, Xu Q N, An W, Qiu R J. Multifunctional coatings crafted *via* layer-by-layer spraying method. *Prog Org Coat* **125**: 215–221 (2018)
[27] Mateos A J, Cain A A, Grunlan J C. Large-scale continuous immersion system for layer-by-layer deposition of flame retardant and conductive nanocoatings on fabric. *Ind Eng Chem Res* **53**(15): 6409–6416 (2014)
[28] Ma D K, Qian S H, Zhou S S, Bian D. Fabrication and characterization of polyelectrolyte coatings by polymerization and co-deposition of acrylic acid using the dopamine in weak acid solution. *Langmuir* **38**(33): 10256–10264 (2022)
[29] Kim K M, Son J H, Kim S K, Weller C L, Hanna M A. Properties of chitosan films as a function of pH and solvent type. *J Food Sci* **71**(3): E119–E124 (2006)
[30] Ma M M, Qi Y H, Gu C J, Zhang Z P. The adsorption behavior of BSA protein on amphiphilic PEG-PS membrane. *Colloid Surface A* **703**: 135282 (2024)
[31] Ash A, Burnett G R, Parker R, Ridout M J, Rigby N M, Wilde P J. Structural characterisation of parotid and whole mouth salivary pellicles adsorbed onto DPI and QCMD hydroxyapatite sensors. *Colloid Surface B* **116**: 603–611 (2014)
[32] Lue S J, Tsai C L, Lee D T, Mahesh K P O, Hua M Y, Hu C C, Jean Y C, Lee K R, Lai J Y. Sorption, diffusion, and perm-selectivity of toluene vapor/nitrogen mixtures through polydimethylsiloxane membranes with two cross-linker densities. *J Membr Sci* **349**(1–2): 321–332 (2010)
[33] Feng X, Xia Y Q, Xie P Y, Li X H. Classification and spectrum optimization method of grease based on infrared spectrum. *Friction* **12**(6): 1154–1164 (2024)
[34] Liu L L, Fu W Y, Wang L L, Shan X B. Dopamine-coated nano-SiO_2-modified PVDF piezoelectric composite film. *New J Chem* **45**(26): 11544–11551 (2021)
[35] Wang R, Xie Y, Xiang T, Sun S D, Zhao C S. Direct catechol conjugation of mussel-inspired biomacromolecule coatings to polymeric membranes with antifouling properties, anticoagulant activity and cytocompatibility. *J Mater Chem B* **5**(16): 3035–3046 (2017)
[36] Gao S J, Sun J C, Liu P P, Zhang F, Zhang W B, Yuan S L, Li J Y, Jin J. A robust polyionized hydrogel with an unprecedented underwater anti-crude-oil-adhesion property. *Adv Mater* **28**(26): 5307–5314 (2016)
[37] Wenzel R N. Resistance of solid surfaces to wetting by water. *Ind Eng Chem* **28**(8): 988–994 (1936)
[38] Nosonovsky M, Bhushan B. Roughness optimization for biomimetic superhydrophobic surfaces. *Microsyst Technol* **11**(7): 535–549 (2005)
[39] Petruczok C D, Armagan E, Ince G O, Gleason K K. Initiated chemical vapor deposition and light-responsive cross-linking of poly (vinyl cinnamate) thin films. *Macromol Rapid Commun* **35**(15): 1345–1350 (2014)
[40] Nguyen T P B, Lee J W, Shim W G, Moon H. Synthesis of functionalized SBA-15 with ordered large pore size and its adsorption properties of BSA. *Micropor Mesopor Mater* **110**(2–3): 560–569 (2008)
[41] Rechendorff K, Hovgaard M B, Foss M, Zhdanov V P, Besenbacher F. Enhancement of protein adsorption induced by surface roughness. *Langmuir* **22**(26): 10885–10888 (2006)
[42] Iqbal M N, Shen Z J, Bengtsson T, Eriksson M. Surface effect of nano-roughened yttria-doped zirconia on salivary protein adhesion. *Materials* **14**(21): 6412 (2021)
[43] Wu X T, Liu Y, Zhang Y L, Wang X W, Yang W F, Jiang L, Ma S H, Cai M R, Zhou F. Interfacial mechanism of hydrogel with controllable thickness for stable drag reduction. *Friction* **12**(2): 231–244 (2024)
[44] Wang G, Ao Q, Gong K, Wang A J, Zheng L, Gong Y D, Zhang X F. The effect of topology of chitosan biomaterials on the differentiation and proliferation of neural stem cells. *Acta Biomater* **6**(9): 3630–3639 (2010)
[45] Qin Y K, Li P C, Guo Z Y. Cationic chitosan derivatives as potential antifungals: A review of structural optimization and applications. *Carbohydr Polym* **236**: 116002 (2020)
[46] Chen D Q, Hu W H. *In situ* investigation of electrochemically mediated surface-initiated atom transfer radical polymerization by electrochemical surface plasmon resonance. *Anal Chem* **89**(8): 4355–4358 (2017)
[47] Lee H, Rho J, Messersmith P B. Facile conjugation of biomolecules onto surfaces via mussel adhesive protein inspired coatings. *Adv Mater* **21**(4): 431–434 (2009)
[48] Song L J, Zhao J, Jin J, Ma J, Liu J C, Luan S F, Yin J H. Fabricating antigen recognition and anti-bioadhesion polymeric surface *via* a photografting polymerization strategy. *Mater Sci Eng C* **36**: 57–64 (2014)
[49] Strola S, Ceccone G, Gilliand D, Valsesia A, Lisboa P, Rossi F. Comparison of surface activation processes for protein immobilization on plasma-polymerized acrylic acid films. *Surf Interface Anal* **42**(6–7): 1311–1315 (2010)

Deke Ma received his bachelor degree in industrial engineering from Shandong Jianzhu University in 2020. He has recently obtained his master degree in mechanical engineering from Jiangnan University. His research interests include biotribology and protein adsorption.

Shanhua Qian received his bachelor, master, and Ph.D. degrees in mechanical engineering from China University of Mining and Technology, in 2003, 2006, and 2009, respectively. After that, he worked as a postdoctoral researcher at the State Key Laboratory of Tribology in Advanced Equipment at Tsinghua University for two years. He joined the School of Mechanical Engineering at Jiangnan University in 2011. His current position is a professor and vice-dean of the School of Mechanical Engineering. His research areas cover the biotribology of soft materials, foods, and coatings as well as bionic design.